nature genetics

# Wnt9b signaling regulates planar cell polarity and kidney tubule morphogenesis

Courtney M Karner[1,2], Rani Chirumamilla[1,2], Shigehisa Aoki[1,3], Peter Igarashi[1,4], John B Wallingford[5] & Thomas J Carroll[1,2]



**Although many vertebrate organs, such as kidneys, lungs and liver, are composed of epithelial tubules, little is known of the mechanisms that establish the length or diameter of these tubules. In the kidney, defects in the establishment or maintenance of tubule diameter are associated with one of the most common inherited human disorders, polycystic kidney disease. Here we show that attenuation of Wnt9b signaling during kidney morphogenesis affects the planar cell polarity of the epithelium and leads to tubules with significantly increased diameter. Although previous studies showed that polarized cell divisions maintain the diameter of postnatal kidney tubules, we find that cell divisions are randomly oriented during embryonic development. Our data suggest that diameter is established during early morphogenetic stages by convergent extension processes and maintained by polarized cell divisions. Wnt9b, signaling through the non-canonical Rho/Jnk branch of the Wnt pathway, is necessary for both of these processes.**

Epithelial and endothelial tubules are some of the most common structures in the vertebrate body plan. Alterations in the shape of these structures have significant impact on their function. For instance, the functional unit of the kidney, the nephron, is a vascularized epithelial tubule whose proper three-dimensional structure is essential for its function in maintaining body fluid composition[1]. Defects in the establishment or maintenance of nephron diameter play causal roles in one of the most common genetic maladies in humans, polycystic kidney disease[2]. Studies in mice and humans have suggested that increased rates of cell proliferation are associated with, and may directly cause, cyst formation[2,3]. However, examination of the developing epithelial tubules of worms and flies indicates that cellular processes that are independent of changes in cell number (for example, cell size, membrane biosynthesis, cell polarity and cell movements) have significant impact on the establishment and maintenance of tubular diameter[4–15].

The *Wnt* genes encode a family of secreted glycolipoproteins that function in multiple biological processes including embryonic development and disease pathogenesis[16]. Previous studies have indicated that tight regulation of Wnt signaling is essential for proper development of the kidney tubules. Loss of canonical Wnt signaling in mice prevents formation of the tubules, and inappropriate activation of the Wnt signal transduction pathway leads to cyst formation[17–19]. In fact, improper stimulation of the canonical Wnt pathway is a hallmark of various types of human cystic kidney diseases[20]. However, recent studies have suggested that defects in planar cell polarity (PCP), a process that may be regulated by noncanonical (β-catenin independent) Wnt signaling, may also contribute to cystogenesis[21].

PCP describes the polarization of cells perpendicular to their apical-basal axis[22]. Genetic screens in *Drosophila* have identified multiple factors that are required for the establishment of PCP including two components of the Wnt pathway, Frizzled (Fz) and Dishevelled (Dsh)[23,24]. Whether Wnt ligands play a direct role in establishing PCP is somewhat controversial[22,25–28].

We previously showed that Wnt9b was necessary for the earliest events in the induction of the kidney tubules[17]. Here we demonstrate that Wnt9b is also required for morphogenesis of the nephron. Wnt9b produced by the ureteric bud and collecting ducts is required autonomously and nonautonomously for proper PCP within the collecting ducts and the adjacent proximal tubules, respectively. Specifically, we show that these tubules develop in two distinct phases. During the first phase, cell division is not oriented but the diameter of the epithelium decreases. We propose that convergent extension-like processes drive the lengthening and thinning of the tubules and establish diameter. In the second phase, polarized cell divisions predominate and maintain tubule diameter. We have found that Wnt9b regulates both phases of development, perhaps through a role in regulating cell orientation. In contrast to its role in tubule induction, Wnt9b's role in tubule morphogenesis is mediated by the noncanonical/PCP signal transduction branch. This study demonstrates that loss of noncanonical Wnt signaling can contribute to cystogenesis and indicates that convergent extension processes regulate tubule diameter in a vertebrate.

[1]Department of Internal Medicine, Division of Nephrology and [2]Department of Molecular Biology, University of Texas Southwestern Medical Center, Dallas, Texas, USA. [3]Pathology & Biodefense Faculty of Medicine, Saga University, Saga, Japan. [4]Department of Pediatrics, University of Texas Southwestern Medical Center, Dallas, Texas, USA. [5]Molecular, Cell and Developmental Biology & Institute for Cellular and Molecular Biology, University of Texas, Austin, Austin, Texas, USA. Correspondence should be addressed to T.J.C. (thomas.carroll@utsouthwestern.edu).

Received 10 June 2008; accepted 29 April 2009; published online 21 June 2009; doi:10.1038/ng.400

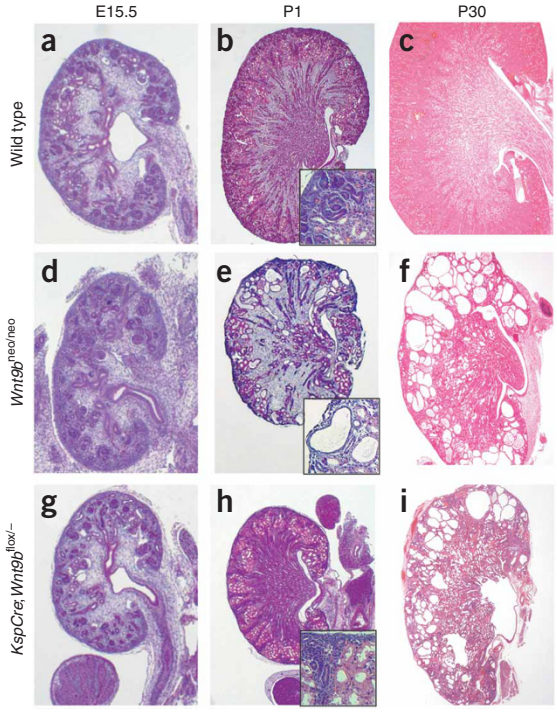


**Figure 1** Defects in Wnt9b signaling results in cyst formation. (**a–i**) Hematoxylin and eosin–stained sections of wild-type (**a–c**), *Wnt9b*$^{neo/neo}$ (**d–f**) and *KspCre;Wnt9b*$^{flox/–}$ (**g–i**) kidneys at E15.5 (**a**,**d**,**g**), P1 (**b**,**e**,**h**) or P30 (**c**,**f**,**i**). Wnt9b mutant kidneys appear normal at E15.5 (compare **d** and **g** to **a**) but are smaller at birth (compare **e** and **h** to **b**). *Wnt9b*$^{neo/neo}$ kidneys also show signs of cystic dysplasia at P1 (**e**). At one month of age, mutant kidneys are slightly smaller and severely cystic compared to wild-type kidneys (compare **f** and **i** to **c**). Insets in **b**, **e** and **h** show high-magnification images of cortical epithelia.

## RESULTS

### Attenuation of Wnt9b signaling leads to dysplastic/cystic kidneys

Embryos completely lacking functional Wnt9b fail to form kidneys, resulting in death on postnatal day 1 (P1). Mice that are homozygous for a hypomorphic (see **Supplementary Note** online) allele of *Wnt9b* (*Wnt9b*$^{neo/neo}$) survive for several days to weeks postpartum (**Fig. 1**) although 100% ($n > 30$) of *Wnt9b*$^{neo/neo}$ animals die within 1 month of birth. Gross examination of a P30 mutant kidney revealed that it contained severely dilated and cystic tubules (**Fig. 1f**), indicating that Wnt9b was required for proper establishment and/or maintenance of tubule diameter.

To test whether the *Wnt9b*$^{neo/neo}$ cystic phenotype was the result of a direct role for Wnt9b in tubule diameter regulation rather than a secondary effect caused by deficits in renal vesicle induction, we attempted to specifically ablate *Wnt9b* from the collecting duct stalks, the cells we hypothesized were the source of Wnt9b during tubule maturation and morphogenesis (for expression of *Wnt9b*, see **Supplementary Fig. 1** online). To accomplish this, we crossed a conditionally inactive (floxed) allele of *Wnt9b* with mice carrying *KspCre*[29]. We found that, similar to what has been described for expression of *Ksp*-cadherin protein (cadh16) in the rabbit[30], the *Ksp* promoter drives expression of Cre recombinase in the collecting duct stalks but not in the ureteric bud tips at least through embryonic day 15.5 (E15.5; **Supplementary Fig. 2** online and data not shown).

Although *Wnt9b* null kidneys do not branch or induce a mesenchymal to epithelial transition[17], *KspCre;Wnt9b*$^{-/flox}$ kidneys form tubules and are indistinguishable from wild-type littermates until at least E15.5 (**Fig. 1g** and **Supplementary Fig. 3** online). However, conditionally mutant mice developed cystic kidneys similar to *Wnt9b*$^{neo/neo}$ mice, although the onset of cystogenesis appeared to be slightly delayed. Although *Wnt9b*$^{neo/neo}$ mice showed signs of tubule dilation as early as E15.5 (data not shown) and had pronounced cysts by P1 (**Fig. 1e** and data not shown), there were few cysts visible in *KspCre;Wnt9b*$^{-/flox}$ kidneys at P1 (**Fig. 1h**). However, cysts were prevalent in *KspCre;Wnt9b*$^{-/flox}$ kidneys at P10, and by P30, there was little normal epithelia remaining (**Fig. 1i** and data not shown).

To further support the hypothesis that Wnt9b had an additional role in kidney tubule morphogenesis, we conducted a temporal knockout of this gene using a ubiquitously expressed, tamoxifen-inducible form of Cre (*CaggCreErTm*)[31]. At 15.5 days postconception, we administered tamoxifen to *Wnt9b*$^{flox/flox}$ dams that had been bred to *CaggCreERTm;Wnt9b*$^{+/–}$ males. When tamoxifen was administered at this time point, the *CaggCreErTm;Wnt9b*$^{-/flox}$ offspring developed cysts and no mutant animals survived past P90 (**Supplementary Fig. 4** online and data not shown). However, ablation of *Wnt9b* after P10 (by administration of tamoxifen to 10-d-old pups) did not have discernible effects on kidney morphology or function when assessed up to one year later (data not shown). These data refute the hypothesis that cyst formation is due to a defect in tubule induction or tubule maintenance. Instead, Wnt9b seems to have an additional, essential function in tubule morphogenesis.

### Wnt9b acts nonautonomously to regulate tubule diameter

*Wnt9b* is expressed in the collecting ducts throughout embryonic development and into adult stages (**Supplementary Fig. 1** and ref. 17). To determine whether Wnt9b is acting to regulate morphogenesis of the collecting ducts or if it is affecting morphogenesis of the adjacent renal vesicle derived epithelia (or both), we determined the origins of the Wnt9b mutant cysts. *Wnt9b*$^{neo/neo}$ and wild-type littermate kidneys were examined with markers of the proximal tubules (*Lotus tetragonolobus* lectin, LTL), collecting ducts (*Dolichos bifloris* agglutinin, DBA) and thick ascending limb of the loop of Henle (Tamm-Horsfall protein, THP) at E15.5, 18.5, P15 and P30.

Marker analysis (**Fig. 2**) suggested that, at E15.5 and P1, cysts were present predominantly in proximal tubules (a tissue that does not express *Wnt9b*) and to a lesser extent in the *Wnt9b*-expressing collecting ducts (**Fig. 2b**,**j** and data not shown). No cysts were found in the loop of Henle or in the glomeruli at or before birth (**Fig. 2f** and data not shown). However, by P15 cysts were present in all nephron segments examined (glomerulus, proximal tubule, loop of Henle and collecting duct) in approximately equal ratios (**Fig. 2d**,**h**,**l** and data not shown). Similar results were seen in P15 *KspCre;Wnt9b*$^{-/flox}$ kidneys (data not shown). These data demonstrate that, after its initial role in tubule induction, Wnt9b functions nonautonomously (and possibly autonomously) to regulate the diameter of kidney tubules.

### Wnt9b is required for polarized cell division in postnatal kidneys

To gain insights into the mechanism underlying cyst formation, we characterized Wnt9b mutant kidneys at the cellular and molecular level. Wnt9b mutant epithelia show no significant differences in their rates of proliferation or apoptosis (**Supplementary Note** and **Supplementary Fig. 5** online). However, recent studies have suggested that cell division is oriented within the plane of the tubular epithelium in postnatal kidneys, and defects in orientation occur in at least five distinct models of PKD[21,32–34]. The noncanonical, or PCP, branch of the Wnt pathway has been implicated in oriented cell division in

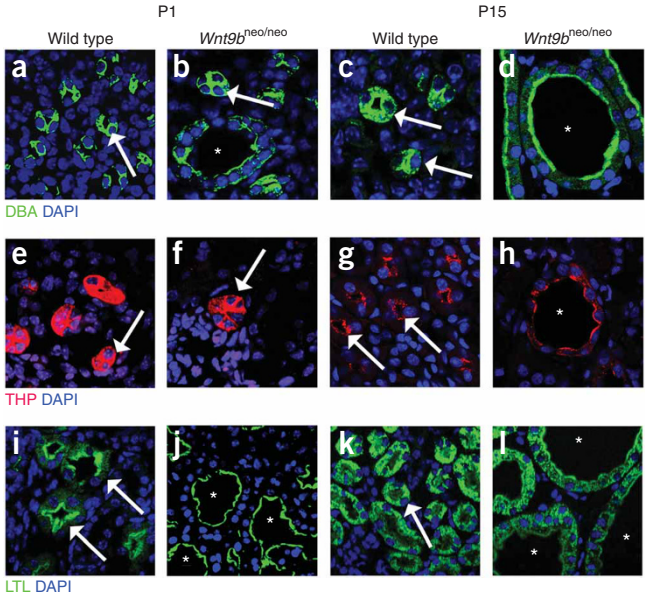


**Figure 2** Characterization of cyst origin in *Wnt9b*$^{neo/neo}$ kidneys. (**a**–**l**) Sections of P1 (**a,b,e,f,i,j**) and P15 (**c,d,g,h,k,l**) kidneys stained with the collecting duct-specific marker *Dolichos biflorus* agglutinin (DBA) (**a**–**d**), the loop of Henle marker Tamm Horsfall protein (THP) (**e**–**h**) and the proximal tubule marker *Lotus tetragolonobus* lectin (LTL) (**i**–**l**). In all panels, arrows denote normal tubules and asterisks denote cystic tubules. At birth, cysts are found primarily in the proximal tubules (compare **i** to **j**). Cysts are also found in the collecting ducts, although the majority of DBA-positive epithelia appear normal (see arrows in **b**). Cysts were not observed in the loop of Henle at birth (compare **e** to **f**). By P15, cysts are present in all segments of the nephron (compare **c** to **b**, **g** to **h** and **k** to **l**). Nuclei were counterstained with DAPI (blue).

gastrulating zebrafish and in worms[25,35]. However, there are several examples, such as the extending *Drosophila* germ band and the developing mouse vasculature endothelium, where oriented cell division seems to be independent of Wnt signaling[36,37]. The mechanism that establishes PCP in the kidney epithelium remains unknown.

To assess whether Wnt9b regulated the orientation of cell division, we measured the orientation of mitotic spindles in the collecting ducts of postnatal kidneys (**Fig. 3** and **Supplementary Fig. 6** online). To avoid complications from examining already cystic epithelia, we initially examined kidneys from the *KspCre;Wnt9b*$^{-/flox}$ line that develops cysts postnatally. We found that, in pre-cystic, P5 *KspCre;Wnt9b*$^{-/flox}$ collecting ducts, cell division was not oriented within the plane of the epithelium (**Fig. 3b**), suggesting that Wnt9b is necessary for the oriented cell divisions that occur in the postnatal kidney. The convoluted nature of the P5 proximal tubule prevented us from collecting accurate data on that segment at that time point.

## Cell division is not oriented in the epithelium of embryonic kidneys

As cysts are present in *Wnt9b*$^{neo/neo}$ kidneys before birth, the mechanism for establishing tubule diameter must be active during embryogenesis. To test whether orientation of cell division played a mechanistic role in the establishment of wild-type tubule diameter, we also measured the orientation of mitotic spindles in straight segments of proximal tubules and collecting ducts at E13.5 and E15.5. Notably, we found that cell division was not oriented within the plane of the tubular epithelium in wild-type collecting ducts or proximal tubules at these times (**Fig. 3a**, **Supplementary Fig. 6a,b** and data not shown). In fact, the distribution of cell divisions was not significantly different from that predicted for a completely random distribution (**Fig. 3a**, **Supplementary Fig. 6a**,**b** and data not shown).

To determine when cell division becomes oriented, we examined mitotic spindles in proximal tubules and collecting ducts at early postnatal stages. We found that, at P1, orientation was no longer random (from a statistical perspective) but also was not tightly oriented within the plane of the epithelium as compared to later postnatal stages (**Supplementary Fig. 6b**). The distribution of mitotic angles in P1 kidneys is roughly biphasic with peaks at 30 and 60 degrees, respectively (**Supplementary Fig. 6b**). There are two possible explanations for this biphasic distribution: either cell division becomes oriented centrifugally (that is from the medulla outward as development proceeds), or there is a general shift toward oriented cell divisions that occurs around the time of birth. To determine whether cell divisions become oriented first in the oldest kidney tubules, we compared mitotic angles between cortical and medullary DBA-positive tubules. The distribution of mitotic angles showed a similar biphasic distribution in both domains, supporting the idea that cell division is becoming oriented throughout the kidney at P1 (**Supplementary Fig. 6c**). As mentioned, at P5, the majority of cell divisions within the collecting duct are well oriented, with 75% of mitotic spindles being oriented within 30 degrees of the longitudinal axis of the tubule (**Fig. 3b** and **Supplementary Fig. 6b**). Once again, because of the convoluted structure of the P5 proximal tubule, we were not able to accurately measure orientation of cell division in this segment. However, similar to the collecting ducts, orientation of cell division in the P1 proximal tubules is no longer random, indicating a trend toward oriented cell division (data not shown).

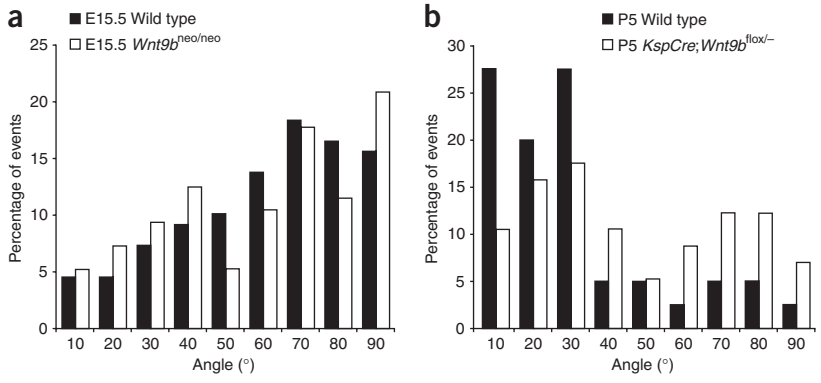


**Figure 3** Cell division becomes oriented after birth in a Wnt9b-dependent process. (**a**) Graphical representation of the angle between the mitotic spindles and the longitudinal axis of DBA-positive tubules at E15.5 indicates that cell division in both wild-type (black bars) and *Wnt9b*$^{neo/neo}$ tubules (white bars) is randomly oriented at E15.5 when compared to the expected random distribution by the Kolmogorov-Smirnov (KS) test. $P > 0.55$ for both wild-type ($n = 109$) and mutant ($n = 96$). (**b**) At P5, the orientation of dividing cells in *KspCre;Wnt9b*$^{-/flox}$ DBA-positive cells (white bars, $n = 50$) is significantly different ($P < 0.01$, Mann-Whitney U test) from wild-type (black bars, $n = 45$), indicating that Wnt9b is necessary for orientation of cell division that occurs postnatally.

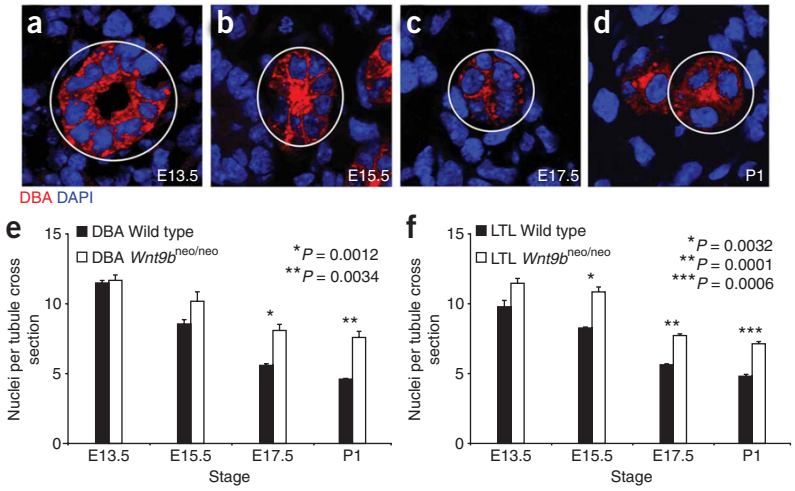


**Figure 4** Wnt9b is required for the elongation and narrowing of kidney tubules. (**a**–**d**) Representative sections through wild type DBA-positive tubules from E13.5 (**a**), E15.5 (**b**), E17.5 (**c**) and P1 mice (**d**) showing the number of nuclei composing the wall of the tubule. Outlined tubules represent transverse sections. Quantitation reveals that the number of cells within the wall of wild-type collecting duct (black bars in **e**; $n = 563$, 606, 844 and 692 for E13.5, 15.5, 17.5 and P1, respectively) and proximal tubules (black bars in **f**; $n = 425$, 1030, 791 and 778 for E13.5, 15.5, 17.5 and P1, respectively) significantly decreases during the embryonic period. The number of cells within the tubule wall is significantly increased in Wnt9b mutant kidneys (white bars in **e** and **f**; $n = 384$ or 412, 521 or 424, 915 or 902, and 665 or 635 for DBA or LTL at E13.5, E15.5, E17.5 or P1, respectively). $n = 3$ kidneys for each stage, tubular segment and genotype. Error bars, s.e.m.



These data suggest that, during embryonic stages, cell divisions are not oriented in the proximal tubules or collecting ducts but that they become oriented, at least within a subset of cells, around the time of birth. Therefore, oriented cell divisions cannot be playing a role in establishment of tubule diameter or in the defects seen in prenatal Wnt9b mutant kidneys. In support of this hypothesis, the orientation of cell division of Wnt9b mutant collecting ducts and proximal tubules was not significantly different from wild-type (that is, it was random) before birth (**Fig. 3a** and **Supplementary Fig. 6a**).

## Kidney tubule diameter decreases during the embryonic period

In the absence of cell loss, cell division that is not oriented within the plane of the tubular epithelium would be predicted to lead to an increase in the number of cells within the tubule wall and, in the absence of changes in cell shape or size, a concomitant increase in cross-sectional tubular diameter. To test whether wild-type tubules increased the number of cells in their walls during the embryonic period, we calculated the average number of cells that make up the circumference of both proximal tubules and collecting ducts (**Fig. 4a–f** and data not shown). Counts were taken from E13.5 (the earliest stage at which we could find both LTL- and DBA-positive tubules) to P1 (before highly oriented cell divisions). Contrary to expectation, we found that the number of cells that make up the tubular circumference decreases by more than half from E13.5 to P1 in both collecting ducts and proximal tubules (**Fig. 4e,f**). The rate of cell loss during this period cannot account for this decrease (**Supplementary Fig. 5b,d** and data not shown), suggesting that some unidentified process must be driving the decrease in the number of cells making up the tubular circumference during the embryonic period.

## Wnt9b mutants show defects in planar cell polarity

One process that could lead to a decrease in the number of cells within the circumference of the tubule without affecting cell number is convergent extension. Convergent extension describes the directed intercalation of cells within an epithelium that makes the epithelium longer and narrower[26,38–43].

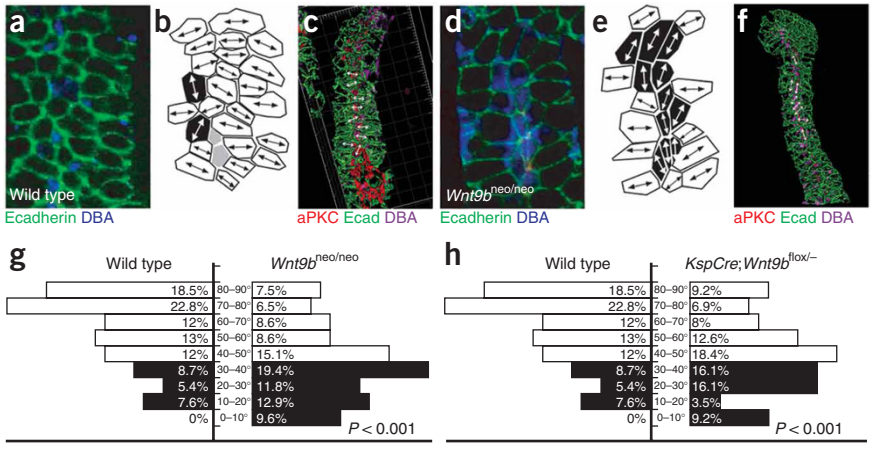


**Figure 5** Wnt9b is necessary for the orientation of polarized cells perpendicular to the axis of extension. (**a**–**f**) Confocal images (**a,d**), cell outlines (**b,e**) and three-dimensional reconstructions (**c,f**) of frontal sections through E15.5 wild-type (**a**–**c**) and *Wnt9b*$^{neo/neo}$ (**d**–**f**) kidneys stained with antibody to E-cadherin (green), antibody to aPKC (red) and DBA (blue). In all cases, proximal is up and distal is down. Images in **a** and **d** represent sections just basal to the apical membrane as marked by antibody to aPKC (red, not seen). Mediolaterally elongated cells are marked in white, proximal-distally elongated cells in black and unelongated cells in gray in **b** and **e**. The majority of wild-type cells are seen to be mediolaterally elongated perpendicular to the axis of extension (white in **b**). *Wnt9b*$^{neo/neo}$ cells are still elongated but the direction of elongation appears to be random (note increased number of black, proximal-distally elongated cells in **e** relative to **b**). (**c,f**) Three-dimensional reconstructions of wild-type (**c**) or *Wnt9b*$^{neo/neo}$ (**f**) E15.5 tubules to allow for visualization of cell orientation. Arrows indicate angle of orientation for marked cells. (**g,h**) Quantitation of the angle of cellular elongation relative to the proximal distal axis of the tubule for wild-type (left in **g** and **h**) and *Wnt9b*$^{neo/neo}$ mutant (right in **g**) or *KspCre;Wnt9b*$^{-/flox}$ (right in **h**) cells. White bars indicate cells that are perpendicular to the axis of elongation (45–90°), whereas black bars represent cells that are parallel (0–45°). The percentage of cells within each 10° increment is indicated. There is a significant change in the orientation of the elongated cells between wild-type and mutants ($P < 0.001$, KS test). The data were gathered from at least three different animals. The total number of oriented cells analyzed is 92, 86 or 93 for wild-type, *KspCre;Wnt9b*$^{flox/-}$ or *Wnt9b*$^{neo/neo}$, respectively. Wild-type cells are from littermate controls.

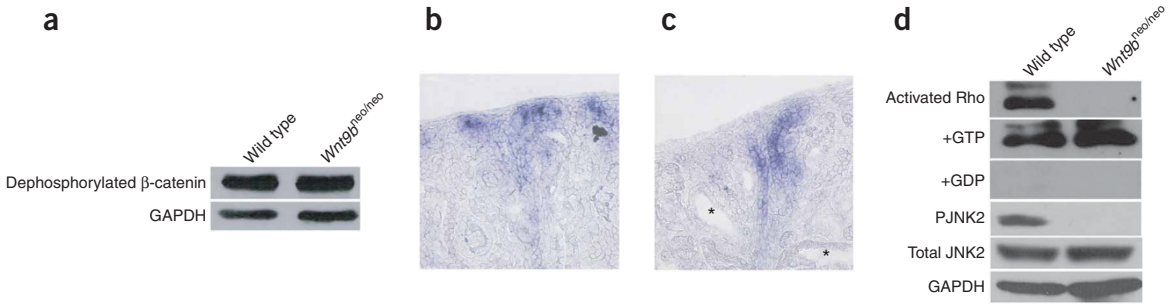


**Figure 6** Wnt9b signals through the noncanonical pathway to regulate tubule diameter. (**a**) Protein blots of total protein extracted from wild-type and *Wnt9b*$^{neo/neo}$ kidneys probed with an antibody specific to the dephosphorylated (active) form of β-catenin show no significant differences in canonical Wnt activity compared to wild-type. (**b**,**c**) Section *in situ* hybridization with a probe for the β-catenin target Axin2 also shows no significant decrease in canonical activity in P1 *Wnt9b*$^{neo/neo}$ kidneys (**c**) compared to wild-type (**b**). Note that there is no ectopic Axin2 expression in cystic proximal tubules (asterisks in **c**). (**d**) Protein blots indicate that activated Rho is significantly decreased in *Wnt9b*$^{neo/neo}$ kidneys at P1 relative to total (+GTP control) Rho levels. Addition of GDP (+GDP) to inactivate Rho was used as a negative control. Phosphorylated Jnk2 is also significantly decreased in *Wnt9b*$^{neo/neo}$ kidneys at P1 relative to total levels of Jnk2. Blots shown are representative examples of data gathered from at least three different blots from three independent protein extractions.



Convergent extension movements rely on dynamic cell shape changes and cell intercalations that are the results of reorganization of the cytoskeleton. Mediolateral elongation of cells perpendicular to the axis of extension is correlated with, and appears necessary for, intercalation of cell during convergent extension in multiple tissues[44–47]. Examination of frontal sections of developing wild-type kidney tubules indicated that the majority of collecting duct cells showed polarized elongation (**Fig. 5** and data not shown) and that greater than 70% of elongated cells were oriented between 45 and 90 degrees (perpendicular) of the longitudinal axis of the tubule (**Fig. 5b**,**g**). Moreover, 41.3% of elongated cells were oriented within 70–90 degrees (**Fig. 5b**,**g**). In contrast, collecting duct cells in *Wnt9b*$^{neo/neo}$ mutants showed a randomized elongation (**Fig. 5d–g** and data not shown). Only 38% of cells in *Wnt9b*$^{neo/neo}$ mutants were elongated within 45–90 degrees and only 14% within 70–90 degrees (**Fig. 5e**,**g**). These defects suggest that Wnt9b has a role in establishing PCP of the kidney epithelium. Similar results were found in the *KspCre;Wnt9b*$^{-/flox}$ mutants (**Fig. 5h**). These data suggest that Wnt9b mutant epithelia have defects in PCP that affect both cell movements and oriented cell divisions.

If defects in polarized cell orientation lead to defects in convergent extension movements, one would predict that the mutant tubules would possess a greater number of cells in their cross sectional circumference. Indeed, this was the case. *Wnt9b*$^{neo/neo}$ mutants had a significantly increased number of cells per tubule wall in the proximal tubules and collecting ducts at E13.5, 15.5, 17.5 and P1 (**Fig. 4e**,**f** and data not shown). Cell size, however, did not seem to be affected (data not shown). It is important to note that the cellular numbers calculated for later stage (E15.5–P1) mutants are most likely an underestimate of true values. To ensure that only epithelial cross sections were evaluated, we did not analyze tubules that varied significantly from being perfect circles (see Online Methods). At later stages, owing to drastically increased diameter, most mutant tubules were grossly misshapen and were excluded from the analysis. Therefore, the mutant tubules assessed are the most 'wild-type' examples, leading to an underestimate of the true number of cells per mutant tubule wall.

### Wnt9b signals through a noncanonical pathway

Although previous studies suggested that Wnt9b signaled through the canonical β-catenin–dependent signal transduction branch during kidney tubule induction[17,18], this pathway seemed to be unaffected in the cystic mutants (**Fig. 6a–c**, **Supplementary Note** and **Supplementary Fig. 7** online). These data suggest that Wnt9b signals through one of the noncanonical pathways to regulate tubule diameter. As the PCP branch of this pathway has previously been implicated in cell orientation and convergent extension movements, we sought to determine whether its activity was affected in Wnt9b mutants. Although there is no established molecular readout of PCP in vertebrates, it has been shown that signaling through this pathway can activate the Rho-GTPases and Jun kinase (Jnk)[48–50]. Activated (GTP-bound) levels of Rho (but not Cdc42 or Rac) were significantly decreased relative to total Rho levels in mutants (**Fig. 6d** and data not shown). Further, we found a significant decrease in the level of phosphorylated Jnk2 (relative to total Jnk2) in P1 Wnt9b mutant kidneys (**Fig. 6d**). These data support the hypothesis that Wnt9b signals through the noncanonical PCP pathway to regulate convergent extension and oriented cell division during kidney tubule morphogenesis.

## DISCUSSION

In this study, we demonstrate that, in addition to its initial role in renal vesicle formation, Wnt9b plays a later role in renal tubule morphogenesis. Mice carrying a hypomorphic mutation of *Wnt9b* or mice that have had a floxed allele of *Wnt9b* deleted with either *KspCre* or the tamoxifen-inducible *CaggCreErTm;Wnt9b*$^{-/flox}$ develop cystic kidneys. Cystogenesis does not seem to be caused by increased cell numbers, as we have not detected differences in the rates of cell proliferation or apoptosis in mutant epithelia either before or concurrent with cyst formation. Instead, we hypothesize that cyst formation is the result of defects in PCP. We show that cells within the epithelial tubule are elongated perpendicular to the proximal-distal axis of the tubule and that this process is dependent on Wnt9b. We hypothesize that proper cell orientation is required for convergent extension movements and oriented cell divisions. Although cells within the normal collecting ducts and proximal tubules of embryonic kidneys divide in a random orientation, the number of cells composing the wall of the tubule decreases during the embryonic period. We hypothesize that convergent extension movements drive the number of cells within the circumference (or wall) of a tubule to decrease as the tubule elongates. This process, at least in part, establishes the tubule diameter and contributes to tubule length. Once the tubule diameter is established, cell division becomes oriented parallel to the proximal-distal axis to ensure that the kidney tubules continue to elongate while they maintain their diameter. Our data suggest that Wnt9b plays essential roles in both of these processes, perhaps by mediating cell orientation.

In stark contrast to its β-catenin–dependent, canonical role during tubule induction[17,18], we have shown that the role of Wnt9b in establishing and maintaining tubule diameter is independent of β-catenin. Instead, Wnt9b seems to signal through the noncanonical Rho/Jnk pathway during tubule morphogenesis. Notably, recent studies showed that attenuation of Rho kinase led to shorter, wider tubules in cultured kidneys[51,52], a phenotype that may reflect attenuation of Wnt9b signaling. Our data support a hypothesis whereby Wnt pathway usage is not determined by the individual ligand but instead by the cellular environment in which the signal is received. Depending on the cell type, Wnt9b can signal through both pathways within the same organ system.

Several factors involved in cystic kidney diseases are localized to, and/or are necessary for the function of, apical monocilia[32,53–64]. In addition, recent studies suggest that the primary cilium may play a role in inhibiting canonical Wnt signaling (perhaps promoting noncanonical Wnt signaling) in early mouse and zebrafish embryos[65,66]. A simple model for Wnt pathway usage in the kidney is that the cilia and/or ciliary factors block canonical signaling by Wnt9b and promote noncanonical signaling. Indeed, we saw no defects in the expression or localization of several ciliary factors such as Pc-1 and Pc-2 (proteins involved in the progression of human autosomal dominant PKD)[61,67] and inversin (*Invs*) mRNA (the ortholog of the gene mutated in nephronophthisis type II)[60] in Wnt9b mutants, nor is *Wnt9b* mRNA expression affected in $Invs^{-/-}$ (ref. 68) or $Pkd1^{-/-}$ (ref. 67) mice (data not shown).

Although this study has revealed a great deal about the mechanisms that regulate tubule diameter, several questions remain unanswered. For example, why Wnt9b mutant cysts are primarily restricted to the cortex of the kidney? There are several possible answers. The simplest is that another molecule compensates for Wnt9b in the medullary region. Several Wnts, including Wnt5a, Wnt7b, Wnt4 and Wnt11, are expressed in the medullary region of both wild-type and Wnt9b mutant kidneys (ref. 69 and C.M.K. and T.J.C., unpublished data) and any one of these factors may compensate for loss of Wnt9b. Alternatively, there may be a parallel, Wnt-independent signaling pathway that regulates PCP in the medulla. A recent study showed that mice lacking the PCP determinant Fat4 developed kidney cysts primarily within the medullary region[34]. Compensation by either another Wnt or Fat4 would explain the paucity of medullary cysts in Wnt9b mutants. However, it is important to note that we did observe increased numbers of cells within the circumference of the Wnt9b mutant collecting ducts as well as defects in cell orientation during embryonic stages but did not observe cysts in this nephron segment until postnatal stages. Similar findings were observed by another study[69], suggesting that other processes such as defects in fluid secretion or cellular growth (hypertrophy) most likely contribute to cyst formation.

Another question raised by these findings concerns how Wnt9b, produced by the collecting ducts, affects PCP in the relatively distant proximal tubules. The simplest hypothesis is that Wnt9b, secreted from the collecting ducts, travels vertically through the stroma to polarize the epithelia. However, it is formally possible that Wnt9b travels through the lumen or through the plane of the epithelium (transcytosis) to regulate morphogenesis. This question is complicated by the fact that we do not know the cell type that is the target of Wnt9b, nor do we know at precisely what step during tubule morphogenesis Wnt9b acts, as evidenced by the disparate onset of cystogenesis in *KspCre;*$Wnt9b^{-/flox}$ and *CaggCreErTm;*$Wnt9b^{-/flox}$ mutants. Our model is that Wnt9b signals relatively late or continuously during tubule morphogenesis. However, it is possible that it Wnt9b establishes polarity early on in the process of tubule formation, acting on the metanephric mesenchyme or renal vesicles. Finally, it is possible that Wnt9b does not signal directly to the epithelial cells, instead directly signaling to the intervening stroma, which secondarily affects morphogenesis. Determining which of these mechanisms is used will be facilitated by the identification of molecular targets of Wnt9b.

A final question that remains is whether Wnt9b contributes to human forms of PKD. Wnt9b continues to be expressed in the adult kidney, suggesting that it may have a role in kidney maintenance and/or repair and that improper regulation of this molecule in adults leads to cystogenesis. For instance, improper activation of canonical Wnt9b activity (or failure to divert Wnt9b signaling through the noncanonical branch) in adult kidneys due to loss of ciliary signaling may play a causal role in cystogenesis. Determining whether this is the case will require simultaneous ablation of Wnt9b in kidneys that lack intact ciliary signaling or in injured kidneys.

In sum, our findings show that Wnt9b, produced by the kidney collecting ducts, nonautonomously regulates morphogenesis of the developing kidney tubules. We suggest that Wnt9b is required for PCP and the PCP-dependent cellular processes of convergent extension and oriented cell division. These processes are in turn required to establish and maintain the tubular diameter and length during the embryonic period but are dispensable in healthy, differentiated tubules. A better grasp of the regulation and downstream targets of Wnt9b will substantially influence our understanding of epithelial tubule morphogenesis and the treatment of polycystic kidney disease.

## METHODS

Methods and any associated references are available in the online version of the paper at http://www.nature.com/naturegenetics/.

*Note: Supplementary information is available on the Nature Genetics website.*


### ACKNOWLEDGMENTS

We thank O. Cleaver for reading and commenting on this manuscript, L. Avery for help with statistical analysis, J. Zhou (Brigham and Women's and Harvard Medical School) for providing us with antibodies to Pc-1 and Pc-2 and the Pkd1 mutant kidneys, M. Taketo (Kyoto University) for providing the beta-catenin exon 3 flox mice, O. Cabello (J.H. Quillen College of Medicine, East Tennessee State University) for providing us with the Invs mutant kidneys, B. Adams, E. Small, J. Shelton and the Molecular Pathology Core for technical assistance and L. James and M. Princena for the urine albumin studies. This work was supported by grants from the American Society for Nephrology, the American Heart Association (0730236N), the Polycystic Kidney Disease Research Foundation, the UAB ARPKD Center (5P30DK07403802) and the US National Institutes of Health (1R01DK080004) to T.J.C. The work was also supported by the University of Texas Southwestern O'Brien Kidney Research Core Center (NIH P30DK079328). J.B.W. was supported by grants from the National Institute for General Medical Sciences, the March of Dimes and the Burroughs Wellcome Fund.


### AUTHOR CONTRIBUTIONS

C.M.K. designed experiments, performed experiments, assembled data and wrote the manuscript, R.C. performed biochemistry, S.A. assisted with quantitative analysis on $Wnt9b^{neo/neo}$ kidneys, P.I. provided *KspCre* mice and commented on manuscript, J.B.W. assisted with cell orientation analysis and T.J.C. performed initial experiments, designed experiments and wrote the manuscript.


Published online at http://www.nature.com/naturegenetics/
Reprints and permissions information is available online at http://npg.nature.com/reprintsandpermissions/



1. Schedl, A. Renal abnormalities and their developmental origin. *Nat. Rev. Genet.* **8**, 791–802 (2007).
2. Torres, V.E., Harris, P.C. & Pirson, Y. Autosomal dominant polycystic kidney disease. *Lancet* **369**, 1287–1301 (2007).
3. Ibraghimov-Beskrovnaya, O. Targeting dysregulated cell cycle and apoptosis for polycystic kidney disease therapy. *Cell Cycle* **6**, 776–779 (2007).
4. Araujo, S.J., Aslam, H., Tear, G. & Casanova, J. mummy/cystic encodes an enzyme required for chitin and glycan synthesis, involved in trachea, embryonic cuticle and

CNS development—analysis of its role in *Drosophila* tracheal morphogenesis. *Dev. Biol.* **288**, 179–193 (2005).
5. Jayaram, S.A. *et al.* COPI vesicle transport is a common requirement for tube expansion in *Drosophila*. *PLoS ONE* **3**, e1964 (2008).
6. Tsarouhas, V. *et al.* Sequential pulses of apical epithelial secretion and endocytosis drive airway maturation in *Drosophila*. *Dev. Cell* **13**, 214–225 (2007).
7. Wang, S. *et al.* Septate-junction-dependent luminal deposition of chitin deacetylases restricts tube elongation in the *Drosophila* trachea. *Curr. Biol.* **16**, 180–185 (2006).
8. Hemphala, J., Uv, A., Cantera, R., Bray, S. & Samakovlis, C. Grainy head controls apical membrane growth and tube elongation in response to Branchless/FGF signalling. *Development* **130**, 249–258 (2003).
9. Jung, A.C., Ribeiro, C., Michaut, L., Certa, U. & Affolter, M. Polychaetoid/ZO-1 is required for cell specification and rearrangement during *Drosophila* tracheal morphogenesis. *Curr. Biol.* **16**, 1224–1231 (2006).
10. Luschnig, S., Batz, T., Armbruster, K. & Krasnow, M.A. *serpentine* and *vermiform* encode matrix proteins with chitin binding and deacetylation domains that limit tracheal tube length in *Drosophila*. *Curr. Biol.* **16**, 186–194 (2006).
11. Lubarsky, B. & Krasnow, M.A. Tube morphogenesis: making and shaping biological tubes. *Cell* **112**, 19–28 (2003).
12. Nishimura, M., Inoue, Y. & Hayashi, S. A wave of EGFR signaling determines cell alignment and intercalation in the *Drosophila* tracheal placode. *Development* **134**, 4273–4282 (2007).
13. Paul, S.M., Palladino, M.J. & Beitel, G.J. A pump-independent function of the Na,K-ATPase is required for epithelial junction function and tracheal tube-size control. *Development* **134**, 147–155 (2007).
14. Wu, V.M. & Beitel, G.J. A junctional problem of apical proportions: epithelial tube-size control by septate junctions in the *Drosophila* tracheal system. *Curr. Opin. Cell Biol.* **16**, 493–499 (2004).
15. Tong, X. & Buechner, M. CRIP homologues maintain apical cytoskeleton to regulate tubule size in *C. elegans*. *Dev. Biol.* **317**, 225–233 (2008).
16. Merkel, C.E., Karner, C.M. & Carroll, T.J. Molecular regulation of kidney development: is the answer blowing in the Wnt? *Pediatr. Nephrol.* **22**, 1825–1838 (2007).
17. Carroll, T.J., Park, J.S., Hayashi, S., Majumdar, A. & McMahon, A.P. Wnt9b plays a central role in the regulation of mesenchymal to epithelial transitions underlying organogenesis of the mammalian urogenital system. *Dev. Cell* **9**, 283–292 (2005).
18. Park, J.S., Valerius, M.T. & McMahon, A.P. Wnt/β-catenin signaling regulates nephron induction during mouse kidney development. *Development* **134**, 2533–2539 (2007).
19. Saadi-Kheddouci, S. *et al.* Early development of polycystic kidney disease in transgenic mice expressing an activated mutant of the β-catenin gene. *Oncogene* **20**, 5972–5981 (2001).
20. Benzing, T., Simons, M. & Walz, G. Wnt signaling in polycystic kidney disease. *J. Am. Soc. Nephrol.* **18**, 1389–1398 (2007).
21. Fischer, E. *et al.* Defective planar cell polarity in polycystic kidney disease. *Nat. Genet.* **38**, 21–23 (2006).
22. Karner, C., Wharton, K.A. Jr. & Carroll, T.J. Planar cell polarity and vertebrate organogenesis. *Semin. Cell Dev. Biol.* **17**, 194–203 (2006).
23. Klingensmith, J., Nusse, R. & Perrimon, N. The *Drosophila* segment polarity gene *dishevelled* encodes a novel protein required for response to the wingless signal. *Genes Dev.* **8**, 118–130 (1994).
24. Vinson, C.R., Conover, S. & Adler, P.N. A *Drosophila* tissue polarity locus encodes a protein containing seven potential transmembrane domains. *Nature* **338**, 263–264 (1989).
25. Goldstein, B., Takeshita, H., Mizumoto, K. & Sawa, H. Wnt signals can function as positional cues in establishing cell polarity. *Dev. Cell* **10**, 391–396 (2006).
26. Heisenberg, C.P. *et al.* Silberblick/Wnt11 mediates convergent extension movements during zebrafish gastrulation. *Nature* **405**, 76–81 (2000).
27. Tada, M. & Smith, J.C. *Xwnt11* is a target of *Xenopus* Brachyury: regulation of gastrulation movements via Dishevelled, but not through the canonical Wnt pathway. *Development* **127**, 2227–2238 (2000).
28. Wehrli, M. *et al. arrow* encodes an LDL-receptor-related protein essential for Wingless signalling. *Nature* **407**, 527–530 (2000).
29. Shao, X., Somlo, S. & Igarashi, P. Epithelial-specific Cre/lox recombination in the developing kidney and genitourinary tract. *J. Am. Soc. Nephrol.* **13**, 1837–1846 (2002).
30. Thomson, R.B. & Aronson, P.S. Immunolocalization of Ksp-cadherin in the adult and developing rabbit kidney. *Am. J. Physiol.* **277**, F146–F156 (1999).
31. Hayashi, S. & McMahon, A.P. Efficient recombination in diverse tissues by a tamoxifen-inducible form of Cre: a tool for temporally regulated gene activation/inactivation in the mouse. *Dev. Biol.* **244**, 305–318 (2002).
32. Jonassen, J.A., San Agustin, J., Follit, J.A. & Pazour, G.J. Deletion of IFT20 in the mouse kidney causes misorientation of the mitotic spindle and cystic kidney disease. *J. Cell Biol.* **183**, 377–384 (2008).
33. Patel, V. *et al.* Acute kidney injury and aberrant planar cell polarity induce cyst formation in mice lacking renal cilia. *Hum. Mol. Genet.* **17**, 1578–1590 (2008).
34. Saburi, S. *et al.* Loss of Fat4 disrupts PCP signaling and oriented cell division and leads to cystic kidney disease. *Nat. Genet.* **40**, 1010–1015 (2008).
35. Gong, Y., Mo, C. & Fraser, S.E. Planar cell polarity signalling controls cell division orientation during zebrafish gastrulation. *Nature* **430**, 689–693 (2004).
36. da Silva, S.M. & Vincent, J.P. Oriented cell divisions in the extending germband of *Drosophila*. *Development* **134**, 3049–3054 (2007).
37. Zeng, G. *et al.* Orientation of endothelial cell division is regulated by VEGF signaling during blood vessel formation. *Blood* **109**, 1345–1352 (2007).
38. Wang, J. *et al.* Regulation of polarized extension and planar cell polarity in the cochlea by the vertebrate PCP pathway. *Nat. Genet.* **37**, 980–985 (2005).
39. Wallingford, J.B., Vogeli, K.M. & Harland, R.M. Regulation of convergent extension in *Xenopus* by Wnt5a and Frizzled-8 is independent of the canonical Wnt pathway. *Int. J. Dev. Biol.* **45**, 225–227 (2001).
40. Torban, E., Wang, H.J., Groulx, N. & Gros, P. Independent mutations in mouse *Vangl2* that cause neural tube defects in looptail mice impair interaction with members of the Dishevelled family. *J. Biol. Chem.* **279**, 52703–52713 (2004).
41. Djiane, A., Riou, J., Umbhauer, M., Boucaut, J. & Shi, D. Role of frizzled 7 in the regulation of convergent extension movements during gastrulation in *Xenopus laevis*. *Development* **127**, 3091–3100 (2000).
42. Goto, T., Davidson, L., Asashima, M. & Keller, R. Planar cell polarity genes regulate polarized extracellular matrix deposition during frog gastrulation. *Curr. Biol.* **15**, 787–793 (2005).
43. Goto, T. & Keller, R. The planar cell polarity gene *strabismus* regulates convergence and extension and neural fold closure in *Xenopus*. *Dev. Biol.* **247**, 165–181 (2002).
44. Marlow, F., Topczewski, J., Sepich, D. & Solnica-Krezel, L. Zebrafish Rho kinase 2 acts downstream of Wnt11 to mediate cell polarity and effective convergence and extension movements. *Curr. Biol.* **12**, 876–884 (2002).
45. Concha, M.L. & Adams, R.J. Oriented cell divisions and cellular morphogenesis in the zebrafish gastrula and neurula: a time-lapse analysis. *Development* **125**, 983–994 (1998).
46. Wallingford, J.B. *et al.* Dishevelled controls cell polarity during *Xenopus* gastrulation. *Nature* **405**, 81–85 (2000).
47. Shih, J. & Keller, R. Cell motility driving mediolateral intercalation in explants of *Xenopus laevis*. *Development* **116**, 901–914 (1992).
48. Habas, R., Dawid, I.B. & He, X. Coactivation of Rac and Rho by Wnt/Frizzled signaling is required for vertebrate gastrulation. *Genes Dev.* **17**, 295–309 (2003).
49. Strutt, D.I., Weber, U. & Mlodzik, M. The role of RhoA in tissue polarity and Frizzled signalling. *Nature* **387**, 292–295 (1997).
50. Boutros, M., Paricio, N., Strutt, D.I. & Mlodzik, M. Dishevelled activates JNK and discriminates between JNK pathways in planar polarity and wingless signaling. *Cell* **94**, 109–118 (1998).
51. Michael, L., Sweeney, D.E. & Davies, J.A. A role for microfilament-based contraction in branching morphogenesis of the ureteric bud. *Kidney Int.* **68**, 2010–2018 (2005).
52. Meyer, T.N. *et al.* Rho kinase acts at separate steps in ureteric bud and metanephric mesenchyme morphogenesis during kidney development. *Differentiation* **74**, 638–647 (2006).
53. Yoder, B.K. *et al.* Polaris, a protein disrupted in orpk mutant mice, is required for assembly of renal cilium. *Am. J. Physiol. Renal Physiol.* **282**, F541–F552 (2002).
54. Yoder, B.K., Hou, X. & Guay-Woodford, L.M. The polycystic kidney disease proteins, polycystin-1, polycystin-2, polaris, and cystin, are co-localized in renal cilia. *J. Am. Soc. Nephrol.* **13**, 2508–2516 (2002).
55. Watanabe, D. *et al.* The left-right determinant Inversin is a component of node monocilia and other 9+0 cilia. *Development* **130**, 1725–1734 (2003).
56. Ward, C.J. *et al.* Cellular and subcellular localization of the ARPKD protein; fibrocystin is expressed on primary cilia. *Hum. Mol. Genet.* **12**, 2703–2710 (2003).
57. Sun, Z. *et al.* A genetic screen in zebrafish identifies cilia genes as a principal cause of cystic kidney. *Development* **131**, 4085–4093 (2004).
58. Baker, S.A., Freeman, K., Luby-Phelps, K., Pazour, G.J. & Besharse, J.C. IFT20 links kinesin II with a mammalian intraflagellar transport complex that is conserved in motile flagella and sensory cilia. *J. Biol. Chem.* **278**, 34211–34218 (2003).
59. Pazour, G.J., San Agustin, J.T., Follit, J.A., Rosenbaum, J.L. & Witman, G.B. Polycystin-2 localizes to kidney cilia and the ciliary level is elevated in orpk mice with polycystic kidney disease. *Curr. Biol.* **12**, R378–R380 (2002).
60. Otto, E.A. *et al.* Mutations in *INVS* encoding inversin cause nephronophthisis type 2, linking renal cystic disease to the function of primary cilia and left-right axis determination. *Nat. Genet.* **34**, 413–420 (2003).
61. Nauli, S.M. *et al.* Polycystins 1 and 2 mediate mechanosensation in the primary cilium of kidney cells. *Nat. Genet.* **33**, 129–137 (2003).
62. Menezes, L.F. *et al.* Polyductin, the PKHD1 gene product, comprises isoforms expressed in plasma membrane, primary cilium, and cytoplasm. *Kidney Int.* **66**, 1345–1355 (2004).
63. Hou, X. *et al.* Cystin, a novel cilia-associated protein, is disrupted in the cpk mouse model of polycystic kidney disease. *J. Clin. Invest.* **109**, 533–540 (2002).
64. Lin, F. *et al.* Kidney-specific inactivation of the KIF3A subunit of kinesin-II inhibits renal ciliogenesis and produces polycystic kidney disease. *Proc. Natl. Acad. Sci. USA* **100**, 5286–5291 (2003).
65. Corbit, K.C. *et al.* Kif3a constrains β-catenin-dependent Wnt signalling through dual ciliary and non-ciliary mechanisms. *Nat. Cell Biol.* **10**, 70–76 (2008).
66. Gerdes, J.M. *et al.* Disruption of the basal body compromises proteasomal function and perturbs intracellular Wnt response. *Nat. Genet.* **39**, 1350–1360 (2007).
67. Lu, W. *et al.* Perinatal lethality with kidney and pancreas defects in mice with a targeted *Pkd1* mutation. *Nat. Genet.* **17**, 179–181 (1997).
68. Simons, M. *et al.* Inversin, the gene product mutated in nephronophthisis type II, functions as a molecular switch between Wnt signaling pathways. *Nat. Genet.* **37**, 537–543 (2005).
69. Yu, J. *et al.* A Wnt7b-dependent pathway regulates the orientation of epithelial cell division and establishes the cortico-medullary axis of the mammalian kidney. *Development* **136**, 161–171 (2009).

## ONLINE METHODS

**Generation of Wnt9b mutant mice and genotyping.** The *Wnt9b*$^{-}$ and *Wnt9b*$^{neo}$ alleles were previously described[17]. The neomycin cassette in *Wnt9b*$^{neo}$ mice was flanked by FLP recombinase target sites (FRT). To generate *Wnt9b*$^{flox}$ mice, *Wnt9b*$^{neo/+}$ animals were crossed to mice carrying a ubiquitously expressed FLP gene. Removal of the neomycin cassette was confirmed by DNA blot. Males and females that had had the neomycin cassette excised were crossed to each to generate *Wnt9b*$^{flox/flox}$ animals. These mice were maintained as a homozygous line. To generate the conditional null kidneys, *KspCre;Wnt9b*$^{+/-}$ males were crossed to *Wnt9b*$^{flox/flox}$ females. Noon of the day of vaginal plugging was considered E0.5.

Genotyping of mice was conducted by digesting a 0.5 cm piece of tail in tail lysis buffer (Viagen) at 55 °C overnight. The floxed and null alleles were amplified in a single reaction using the conditions previously described[17]. The null allele generates a 500-bp band, the flox allele a 240-bp band and the wild-type allele a 200-bp band. *KspCre* and *CaggCreERTM* alleles were amplified using primers CCATGAGTGAACGAACCTGG and TGATGAGGTTCGCAA GAACC to give a 400-bp band using the conditions previously described. The β-catenin exon3flox mice were provided by Mark Taketo (Kyoto University)[70], and the exon3flox allele was amplified using primers AACT GGCTTTTGGTGTCGGG and TCGGTGGCTTGCTGATTATTTC. Using a 55 °C extension, we obtained a 291-bp band for the wild-type allele and a 400-bp band for the exon-3-floxed allele.

**Immunohistochemistry.** Specimens were fixed in 4% paraformaldehyde in PBS (EMS) for 16 h at 4 °C, washed three times with PBS and cryoprotected in 30% sucrose for 16 h at 4 °C. Specimens were then embedded in OCT and cryosectioned at the thicknesses indicated. Immunohistochemistry was performed as previously described[71]. We examined specimens by scanning laser confocal microscopy (Zeiss LSM-510). Sections were stained with the following lectins or antibodies: *Dolichos bifloris* lectin (DBA, Biotinylated, 1:500 Vector Laboratories), *Lotus Tetragonolobus* lectin (LTL, Biotinylated, 1:500 Vector Laboratories), anti-Laminin (Rabbit polyclonal, 1:300 Sigma), anti-Tamm-Horsfall protein (Rabbit, 1:300 Biomedical Technologies), anti-E-cadherin (Rat, 1:500 Zymed), anti-Ki67 (Rabbit, 1:800 Novocastra), anti-cleaved caspase-3 (Rabbit, 1:300 Promega), anti-GFP (Rabbit, 1:1000 Abcam), anti aPKC (Rabbit, 1:500 Santa Cruz) and Sytox Green (1:5000, Invitrogen).

**Protein blotting.** Wild-type and *Wnt9b*$^{neo/neo}$ (P1) kidneys were homogenized in a medium containing 20 mM Hepes (pH 7.4), 10 mM NaCl, 1.5 mM $MgCl_2$, 20% glycerol, 0.1% Triton X-100, 1 mM DTT, 1.5 mM sodium orthovanadate and protease inhibitor mix (Complete Mini, one protease inhibitor cocktail tablet per 20 ml of medium; Roche Molecular Biochemicals, catalog no. 04693124001) in a dounce homogenizer by giving 40 strokes. The lysate was centrifuged at 905*g* for 3 min in 4 °C to separate the cytosolic and nuclear fractions. Supernatant was used as the cytosolic fraction. Protein concentration was estimated by the Bradford method.

Protein (50 μg) was resolved on 10% polyacrylamide gel and subjected to immunoblot analysis using the respective antibodies. GAPDH was used as a loading control. Antibodies against pJnk1/2 (1:500 dilution, Biosource, catalog no. 44-682G), total Jnk2 (1:1000 dilution, Cell signaling Technology, catalog no. 4672), dephosphorylated β-catenin (1:1000 dilution, Upstate Cell signaling solutions, catalog no. 05-601) and GAPDH (1:3000 dilution, Santa Cruz Biotechnology, catalog no. sc25778) were used to detect the respective protein levels in wild-type and *Wnt9b*$^{neo/neo}$ cytosolic fractions. The immunoblots were blocked for one hour at room temperature in 5% nonfat dry milk (1× TBS, 0.05% Tween) followed by an overnight incubation at 4 °C in their respective diluted primary antibody solutions. Membranes were then washed three times using TBS/Tween 0.05% (5 min/15 ml) and further incubated with the secondary antibody, HRP goat anti-rabbit (Invitrogen, catalog no. G21234) in 5% nonfat dry milk (1× TBS/Tween 0.05%) for 1 h at room temperature (1:5000 to detect pJnk1/2, 1:2000 to detect total Jnk2 and 1:10,000 to detect GAPDH levels). Dephosphorylated β-catenin was detected using HRP goat anti-mouse (1:5000, Pierce, catalog no. 1858413) using the same conditions as described above. All the blots were developed using the Pierce Super signal West Femto maximum sensitivity substrate kit. We quantified protein levels using Image J software and did each experiment was done a minimum of three times with at least two independently prepared protein samples.

**Rho pulldown.** Activated Rho was pulled down from wild-type and *Wnt9b*$^{neo/neo}$ P1 kidneys using EZ-DetectRho Activation Kit with slight modification to the manufacturer's protocol (Pierce, catalog no. 89854). The kidneys were homogenized in the lysis buffer provided in the kit with the addition of protease inhibitor mix (Complete Mini, one protease inhibitor cocktail tablet per 10 ml of medium, Roche Molecular Biochemicals, catalog no. 04693124001) in a dounce homogenizer by giving 10–15 strokes. The lysate was centrifuged at 15,339*g* at 4 °C for 10 min. Supernatant was separated and used for the assay. We used 1 mg of protein for each pull down assay. *In vitro* control treatments were done by the addition of GTP (positive control) or GDP (negative control) to activate or inactivate Rho, respectively.

Protein was resolved on 12% polyacrylamide gel and subjected to immunoblot analysis using antibody to Rho. The immunoblots were blocked in TBS containing 3% BSA at room temperature for 2 h followed by an overnight incubation in primary antibody solution (1:500 dilution in 3% BSA in TBS/Tween-0.05%) at 4 °C. Membranes were washed three times using 15 ml of TBS/Tween-0.05% (5 min each wash) and further incubated with the secondary antibody, HRP goat anti-mouse (Invitrogen, catalog no. G21040) in 5% NFDM (1× TBS/Tween 0.05%) for 1 h at room temperature (1:10000 dilution). Immunoblots were developed using Pierce Super signal West Femto maximum sensitivity substrate kit.

***In situ* hybridization.** *In situ* hybridization was performed on 30 or 16 μm cryosectioned kidneys as previously described[17]. Sections labeled with DBA lectin where washed three times in PBS after the color reaction, fixed in 4% paraformaldehyde in PBS (EMS) for 1 h at room temperature, washed three times with PBS and processed for immunohistochemistry as described previously[71]. Kidneys stained for X-gal were fixed (1% PFA, 0.2% gluteraldehyde in PBS) for 1 h, washed three times with 0.02% NP-40/PBS, stained (5 mM $K_3Fe(CN)_6$, 5 mM $K_4Fe(CN)_6$, 2 mM $MgCl_2$, 0.01% sodium deoxycholate, 0.02% NP-40, 1 mg/ml X-gal) for up two 2 h at 37 °C. Staining was stopped by washing in PBS followed by fixation in 4% PFA + 0.2% gluteraldehyde for 30 min. Samples were then processed for whole-mount *in situ* hybridization as previously[17]. Sections to be stained for X-gal were fixed as for whole-mount staining and processed for cryosectioning as described above. Fourteen-micrometer sections were washed three times with PBS and stained for β-galactosidase activity for a maximum of 1 h at 37 °C. Staining was stopped by washing three times for 10 min in PBS followed by a 10 min fixation in 4% PFA before proceeding to section *in situ* hybridization.

**Tubule diameter counts.** To quantify the number of cells making up the cross-sectional wall of individual tubules, we stained 10-μm kidney sections with segment-specific markers (DBA or LTL), antibodies to the extracellular matrix protein laminin and the nuclear marker 4,6-diamidino-2-phenylindole (DAPI). For the collecting ducts, we excluded the cortical-most epithelia to avoid branching tubules. To ensure that only cross-sections were being analyzed, we measured the diameter of the tubule at two intersecting lines that were perpendicular to each other. If the two measured diameters varied by more than 10% (making the shape of tubule more of an oval than a circle), the section was assumed to be frontal and therefore excluded from analysis. If a tubule was considered to be transverse, the number of nuclei in the tubular cross-section was averaged. This was done for both the collecting ducts and the proximal tubules at multiple embryonic and postnatal time points (E13.5, 15.5, 17.5 and P1). Statistical differences between wild-type and mutants were assessed by Student's *t*-test.

**Measuring the orientation of cell division.** To evaluate the orientation of cell division, we used a protocol similar to that described by previously[21] with slight modification. We labeled 50-μm thick E13.5, 15.5, P1 and P5 kidney sections with an antibody to laminin, a tubule-specific marker (DBA or LTL) and Sytox green. For the collecting ducts, we excluded the cortical-most epithelia to avoid branching tubules. Labeled tubules containing anaphase nuclei were identified and a Z-stack was taken using the Zeiss LSM-510. These images where reconstructed using the Imaris software and Cartesian coordinates were assigned for the mitotic spindles and basal lamina of the tubule (**Supplementary Fig. 6d,e**).

The angle between the resulting vectors was determined according to a method described previously[21]. The randomness of cell division was determined by the Kolmogorov-Smirnov Goodness-of-fit Test.

**Measurement of cell elongation and orientation.** To determine whether cells were elongated, we stained sections of E15.5 kidneys with DBA, E-cadherin and aPKC. The cortical most epithelia were excluded to avoid branching tubules. Z stacks were captured and sections were identified that were frontal through the collecting duct and that fell one frame below (basal to) the aPKC staining. Using Image ProPlus software, two roughly parallel lines were drawn on opposite sides of every cell in the image where E-cadherin staining outlined the entire cell (cells on the edges that had discontinuous E-cadherin staining were not measured). The software then calculated the average distance between those two lines and assigned a length-to-width ratio for each individual cell, with the length being the longer of the two sides. Cells that possessed a length-to-width ratio of greater than 1.2 were considered elongated. To measure the orientation of elongated cells, we assigned a vector for the elongated axis of the cell and the elongated axis of the tubule. The angle between these two vectors was determined using Image ProPlus software. The percentage of total cells that fell within each 10° bin was calculated. Statistical analysis for the wild-type and mutant populations was done according to the Mann-Whitney U test.

70. Harada, N. *et al.* Intestinal polyposis in mice with a dominant stable mutation of the β-catenin gene. *EMBO J.* **18**, 5931–5942 (1999).
71. Marose, T.D., Merkel, C.E., McMahon, A.P. & Carroll, T.J. β-catenin is necessary to keep cells of ureteric bud/Wolffian duct epithelium in a precursor state. *Dev. Biol.* **314**, 112–126 (2008).




doi:10.1038/ng.400